N.I. Pavlyshche [1], A.V. Korotun [1, 2], V.P. Kurbatsky [1]

OPTICAL ABSORPTION OF COMPOSITES WITH METALLIC NANOSIZED SPHEROIDAL PARTICLES

[1] National University "Zaporizhzhia Polytechnic"
64 Zhukovsky Str., Zaporizhzhia, 69063, Ukraine, E-mail: andko@zp.edu.ua
[2] G.V. Kurdyumov Institute for Metal Physics of National Academy of Sciences of Ukraine
36 Academician Vernadsky Blvd., Kyiv, 03142, Ukraine

The paper considers the problem of light absorption by a nanocomposite with randomly oriented metal spheroidal particles-inclusions, provided that the volume content of such inclusions is small. Expressions for the frequency dependences of the effective dielectric function and the absorption coefficient of the metal-dielectric nanocomposite are obtained within the effective medium model taking into account the axial symmetry of spheroidal inclusions. The effective relaxation rate of electrons is introduced using the kinetic approach. Numerical calculations are performed for the cases when inclusion particles have the form of prolate and oblate nanospheroids. The results of the calculations indicate the presence of two maxima of the absorption coefficient, which correspond to longitudinal and transverse surface plasmon resonance. The change in the position and magnitude of the maxima of the frequency dependences of the effective dielectric function and the absorption coefficient with varying the size and shape of the spheroidal particles-inclusions is analyzed. It is shown that the greater the difference in the lengths of the semi-axes of the spheroids, the greater the distance between the maxima of the effective dielectric function and the absorption coefficient, and the shape of the curves depends on the eccentricity of spheroidal inclusions. It has been found that the position of the maxima is significantly influenced by the choice of the material of the inclusion particles and the matrix medium, while the height of the maxima is largely influenced by the shape of the nanoparticles, as well as their volume content in the composite medium. It is proved that, dependent on the material of nanoparticles-inclusions, both maxima of the absorption coefficient can be found in the visible part of the spectrum (for Au inclusions) or in the ultraviolet (for Al inclusions). It is also possible that one maximum lies in the visible part of the spectrum, and the other in the ultraviolet, which is the case for inclusions of Pd, Pt, Cu, Ag.

Keywords: *nanocomposite, prolate and oblate spheroids, effective dielectric function, absorption coefficient, effective relaxation rate*

INTRODUCTION

Nanoclusters and nanoparticles are of interest due to their unusual properties compared to their bulk counterparts. The change in the properties of materials on a nanometer scale is associated with a large ratio of surface area to volume and their morphology. Clusters and nanoparticles are usually very unstable and prone to aggregation. The inclusion or embedding of clusters and nanoparticles in the matrix environment solves this problem [1–4]. The properties of embedded nanoparticles depend on the properties of the matrix and the "matrix-guest" interaction [5].

Optical metal-dielectric nanocomposites are defined as composite materials in which the matrix is a dielectric, and the metal inclusion particles have nanometer dimensions. Dielectrics are suitable matrix media for growing nanoparticles due to their characteristics such as ease and cheapness of processing, high mechanical strength, high optical transparency and chemical stability [6, 7]. The properties of the nanocomposites depend on the matrix material and size, shape, orientation of inclusion particles, as well as on their concentration. Nanocomposites exhibit a strong interaction of inclusion particles with the separation boundary due to the large free surface energy of the dispersed phase. In addition, the properties of nanoparticles embedded in dielectric matrices are influenced by quantum confinement effects. Thus, nanoparticles can significantly change the mechanical, thermal, electrical, optical, chemical and surface properties of dielectric matrices [8].

Metal-dielectric nanocomposites are of great interest due to a significant number of their potential applications in fields such as optoelectronics, photonics, sensors, electrochemistry, catalysis, biomedicine and art [9, 10], laser generation [11], optical computing

and data storage [12], gas sensors [13], printing [14] and solid coatings [15]. The size, shape, volume content and size distribution of nanoparticles determine the efficiency of metal-dielectric composites in all these areas.

The optical response of nanocomposites can be tuned by changing the shape, volume concentration [16] and mutual arrangement [17] of nanoparticles, i.e. controlling Mie-type and plasmonic resonances [18, 19]. These resonances significantly amplify the electromagnetic fields in the immediate vicinity of the nanoparticles. Although the development of technologies has made it possible to manufacture nanocomposites with individual properties [16, 20, 21], a consistent description of their optical properties is still missing. It should be noted that the optical properties of composites with two-layer spherical nanoparticles were considered in works [22, 23].

It is known that in metal-dielectric composites under the action of laser radiation, spherical metal inclusions can be deformed into spheroids. In this regard, and for other reasons mentioned above, the study of light absorption by nanocomposites with spheroidal inclusions is an urgent task.

BASIC RELATIONSHIPS

Consider a metal-dielectric composite, the matrix medium of which has permittivity ϵ_m, and the inclusions are randomly oriented spheroidal metal nanoparticles.

The frequency dependence of the absorption coefficient of such a composite is determined by the relation

$$\eta = \frac{2\omega}{c\sqrt{\epsilon_m}} \, \mathrm{Im}\sqrt{\epsilon_{eff}} \; , \qquad (1)$$

where ω and c are the frequency and velocity of light, respectively.

We will assume that the volume content of metal inclusions is small ($\beta \ll 1$). In this case, the effective dielectric function of the nanocomposite has the form [24]

$$\epsilon_{eff} = \frac{(1-\beta)\epsilon_m + \frac{1}{3}\beta\sum\limits_{i=1}^{3}\vartheta_i\epsilon_i}{1-\beta+\frac{1}{3}\beta\sum\limits_{i=1}^{3}\vartheta_i} \; , \qquad (2)$$

where

$$\vartheta_i = \frac{\epsilon_m}{\epsilon_m + \mathcal{L}_i\left(\epsilon_i - \epsilon_m\right)} \; , \qquad (3)$$

$\mathcal{L}_i$ are depolarization factors of the spheroids, ϵ_i are diagonal components of the dielectric tensor.

Taking into account the axial symmetry, we represent the relations (2) and (3) as follows

$$\epsilon_{eff} = \frac{(1-\beta)\epsilon_m + \frac{1}{3}\beta\left(2\vartheta_\perp\epsilon_\perp + \vartheta_\parallel\epsilon_\parallel\right)}{1-\beta+\frac{1}{3}\beta\left(2\vartheta_\perp + \vartheta_\parallel\right)} \; ; \qquad (4)$$

$$\vartheta_{\perp(\parallel)} = \frac{\epsilon_m}{\epsilon_m + \mathcal{L}_{\perp(\parallel)}\left(\epsilon_{\perp(\parallel)} - \epsilon_m\right)} \; . \qquad (5)$$

Within the Drude model, components of the dielectric tensor of the inclusion particles have the form

$$\epsilon_{\perp(\parallel)}(\omega) = \epsilon^\infty - \frac{\omega_p^2}{\omega\left(\omega + i\gamma_{eff}^{\perp(\parallel)}\right)} \; , \qquad (6)$$

where ϵ^∞ is the contribution of the crystal lattice; $\omega_p = \left(e^2 n_e / \epsilon_0 m^*\right)^{1/2}$ is the plasma frequency, n_e is the concentration of conduction electrons, m^* is the effective mass of electrons, ϵ_0 is the electrical constant. The effective relaxation rate is

$$\gamma_{eff}^{\perp(\parallel)} = \gamma_{bulk} + \gamma_s^{\perp(\parallel)} + \gamma_{rad}^{\perp(\parallel)} \; , \qquad (7)$$

where $\gamma_{bulk} = \mathrm{const}$ is the volume relaxation rate,

$$\gamma_s^{\perp(\parallel)} = \frac{9}{16}\frac{\mathcal{L}_{\perp(\parallel)}}{\epsilon_m + \mathcal{L}_{\perp(\parallel)}\left(1-\epsilon_m\right)}\frac{v_F}{2a}\left(\frac{\omega_p}{\omega}\right)^2 \mathscr{F}_{\perp(\parallel)}\left(e_p\right) \qquad (8)$$

is the rate of surface relaxation,

$$\gamma_{rad}^{\perp(\parallel)} = \frac{V}{8\pi}\frac{\mathcal{L}_{\perp(\parallel)}}{\sqrt{\epsilon_m\left(\epsilon^\infty + \frac{1-\mathcal{L}_{\perp(\parallel)}}{\mathcal{L}_{\perp(\parallel)}}\epsilon_m\right)}}\frac{v_F}{2a}\left(\frac{\omega_p}{\omega}\right)^2\left(\frac{\omega_p}{c}\right)^3 \mathscr{F}_{\perp(\parallel)}\left(e_p\right) \qquad (9)$$

is the radiative damping.

In formulas (8) and (9) v_F is the Fermi velocity of electrons; $V = 4\pi a^2 b/3$ is the volume of a spheroidal particle, a and b are the minor (major) and major (minor) semi-axes of an prolate (oblate) spheroid.

Eccentricities and depolarization factors [25] are determined by the formulas:

$$e_p = \frac{\sqrt{b^2 - a^2}}{b}, \tag{10}$$

$$\mathcal{L}_\parallel = \frac{1 - e_p^2}{e_p^3}\left(\ln\frac{1 + e_p}{1 - e_p} - 2e_p\right),$$

$$\mathcal{L}_\perp = \frac{1}{2}\left(1 - \mathcal{L}_\parallel\right) \tag{11}$$

for a prolate spheroid;

$$e_p = \frac{\sqrt{a^2 - b^2}}{b}; \tag{12}$$

$$\mathcal{L}_\parallel = \frac{1 + e_p^2}{e_p^3}\left(e_p - \text{arctg}\, e_p\right),$$

$$\mathcal{L}_\perp = \frac{1}{2}\left(1 - \mathcal{L}_\parallel\right) \tag{13}$$

for an oblate spheroid.

Size-dependent functions introduced in (8) and (9) are

$$\mathscr{F}_\perp(e_p) = \frac{1}{e_p^3}\left\{e_p\sqrt{1 - e_p^2}\left(\frac{1}{2} + e_p^2\right) + \right.$$

$$\left. + 2\left(e_p^2 - \frac{1}{2}\right)\left(\frac{\pi}{2} - \arcsin\sqrt{1 - e_p^2}\right)\right\}, \tag{14}$$

$$\mathscr{F}_\parallel(e_p) = \frac{1}{e_p^3}\left\{\frac{\pi}{2} - \arcsin\sqrt{1 - e_p^2} + \right.$$

$$\left. + e_p\sqrt{1 - e_p^2}\left(2e_p^2 - 1\right)\right\} \tag{15}$$

for a prolate spheroid;

$$\mathscr{F}_\perp(e_p) = \frac{1}{2e_p^3}\left\{e_p\sqrt{e_p^2 - 1}\left(2e_p^2 - 1\right) + \right.$$

$$\left. + \left(4e_p^2 + 1\right)\ln\left(e_p + \sqrt{e_p^2 - 1}\right)\right\}, \tag{16}$$

$$\mathscr{F}_\parallel(e_p) = \frac{1}{e_p^3}\left\{e_p\sqrt{e_p^2 - 1}\left(2e_p^2 + 1\right) - \ln\left(e_p + \sqrt{e_p^2 - 1}\right)\right\} \tag{17}$$

for an oblate spheroid.

Formulas (1)–(17) were used for numerical calculations, the results of which are given below.

RESULTS OF CALCULATIONS AND THEIR DISCUSSION

Calculations were performed for a composite with nanoparticles of different metals, which have the shape of prolate and oblate spheroids and are in different matrix environments. The parameters of the metals and dielectrics are given in the Table 1 and Table 2, respectively.

Table 1. Parameters of metals (see, for example, [26, 27] and references therein)

Parameters / Metals	Au	Ag	Cu	Pd	Pt	Al
n_e, 10^{22} cm^{-3}	5.91	5.85	17.2	2.53	9.1	18.2
ϵ^∞	9.84	3.70	12.03	2.52	4.42	0.7
$\hbar\omega_p$, eV	9.07	9.17	12.6	9.7	15.2	15.4
$\hbar\gamma_{bulk}$, eV	0.023	0.016	0.024	0.091	0.069	0.082
v_F, 10^6 m/s	1.41	1.49	1.34	2.84	2.98	1.91

Table 2. Dielectric permittivity of matrices (see, for example, [27] and references therein)

Substance	CaF$_2$	Teflon	Al$_2$O$_3$	TiO$_2$	C$_{60}$
ϵ_m	1.54	2.3	3.13	4.0	6.0

Fig. 1 shows the frequency dependences of the real and imaginary parts of the effective dielectric function of the composite with silver particles-inclusions in the form of prolate spheroids in Teflon. Note that $\text{Re}\epsilon_{\text{eff}}(\hbar\omega)$ is an alternating function of the frequency, while $\text{Im}\epsilon_{\text{eff}}(\hbar\omega) > 0$ in the entire studied frequency interval. In addition, the functions $\text{Im}\epsilon_{\text{eff}}(\hbar\omega)$ have two maxima, the distance between which decreases as the difference between the major

and minor semi-axes of the spheroid decreases. This fact can be explained as follows. The maximum values of $\mathrm{Im}\epsilon_{\mathrm{eff}}(\hbar\omega)$ correspond to the surface plasmon resonance frequencies, and there are two such resonances in spheroidal particles. As the shape of the particle approaches spherical, the distance between the resonances decreases, and for a spherical particle these resonances merge into one. It should also be noted that curves *1* and *4* on graphs $\mathrm{Re}\epsilon_{\mathrm{eff}}(\hbar\omega)$ and $\mathrm{Im}\epsilon_{\mathrm{eff}}(\hbar\omega)$ practically coincide, which is related to the equality of the semi-axis ratios (equal eccentricities) in these cases.

Similar dependences for the case when the inclusion particles have the shape of oblate spheroids are shown in Fig. 2. All the discovered facts regarding dependencies $\mathrm{Re}\epsilon_{\mathrm{eff}}(\hbar\omega)$ and $\mathrm{Im}\epsilon_{\mathrm{eff}}(\hbar\omega)$ for inclusion particles in the form of

an prolate spheroid (change in sign, the number and location of maxima, effect of eccentricity) also take place for composites with particles in the form of oblate spheroids.

The frequency dependences of absorption coefficients for composites with inclusions in the form of prolate and oblate spheroids are shown in Fig. 3. The results of the calculations indicate that the maxima of the absorption coefficient in both cases behave like the maxima of the imaginary part of the effective dielectric function, namely, when the shape of the inclusion particles approaches spherical, the maxima converge. It should also be noted that the maximum values of the absorption coefficient are greater in the case when the inclusions are oblate nanospheroids.
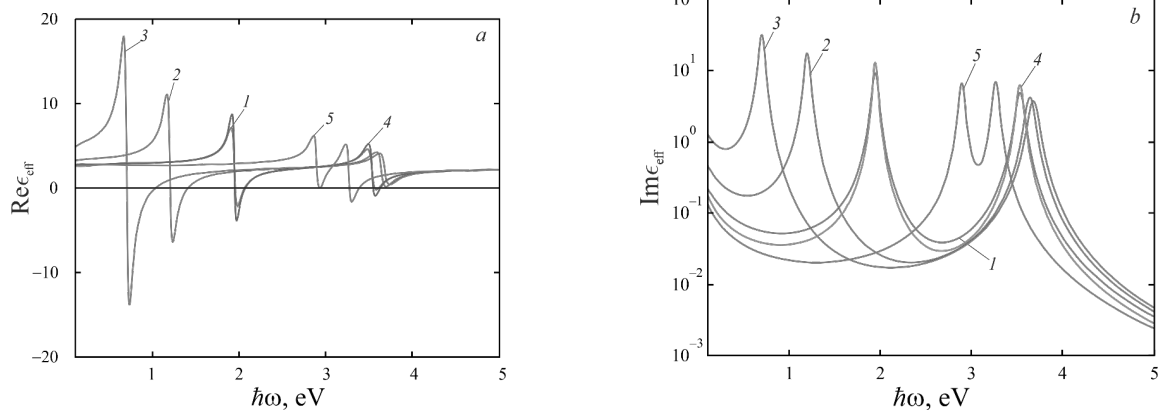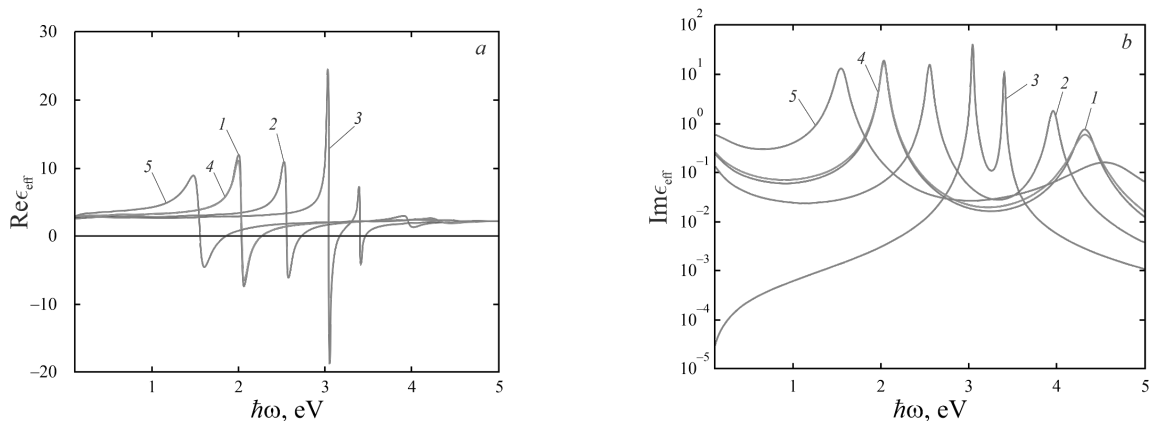

Fig. 1. Frequency dependences of the real (*a*) and imaginary (*b*) parts of the effective dielectric function of the nanocomposite with inclusions in the form of prolate spheroids: *1* – $a_t = 10$ nm, $b_l = 50$ nm; *2* – $a_t = 10$ nm, $b_l = 100$ nm; *3* – $a_t = 10$ nm, $b_l = 200$ nm; *4* – $a_t = 20$ nm, $b_l = 100$ nm; *5* – $a_t = 40$ nm, $b_l = 100$ nm

Fig. 2. Frequency dependences of the real (*a*) and imaginary (*b*) parts of the effective dielectric function of the nanocomposite with inclusions in the form of oblate spheroids: *1* – $a_t = 50$ nm, $b_l = 10$ nm; *2* – $a_t = 50$ nm, $b_l = 20$ nm; *3* – $a_t = 50$ nm, $b_l = 40$ nm; *4* – $a_t = 100$ nm, $b_l = 20$ nm; *5* – $a_t = 200$ nm, $b_l = 20$ nm
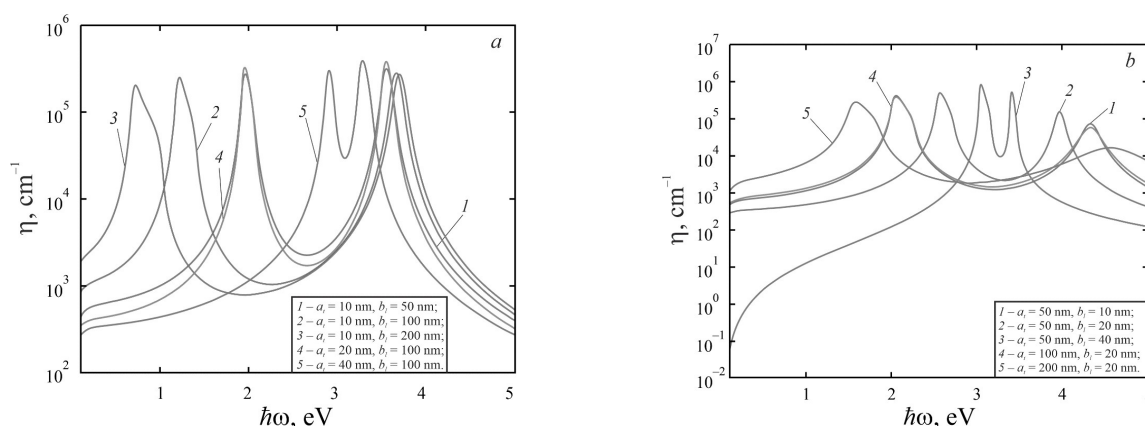
Fig. 3. Frequency dependences of the absorption coefficient of the composite with silver nanoparticles in Teflon in the form of prolate (*a*) and oblate (*b*) spheroids of different sizes

Fig. 4 shows the frequency dependences of the absorption coefficient of the composite with nanoparticles of various metals, which have the shape of prolate and oblate spheroids. Note that the frequencies corresponding to the maxima of these curves are significantly different, which is associated with a significant difference in such metal parameters as the plasma frequency and the contribution of the crystal lattice to the dielectric function. At the same time, depending on the metal of inclusions, three variants of the location of the maxima are possible: both of them in the visible part of the spectrum (when the inclusions are gold nanospheroids), both in the ultraviolet (inclusions of aluminum), and one each in different spectral ranges (inclusions of Pd, Pt, Cu, Ag). The frequencies corresponding to the first maximum in the cases of inclusions in the form of prolate (Fig. 4 *a*) and oblate

(Fig. 4 *b*) spheroids are close, while the frequency of the second maximum is higher, and the maximum value is two orders of magnitude lower when the inclusions are flattened spheroids.

The dependence $\eta(\hbar\omega)$ curves for different matrix media are shown in Fig. 5. The results indicate a "blue" shift when permittivity of the matrix decreases. Regarding the location and height of the first and second maxima, note a full agreement with the patterns discussed above.

The results of calculations of the absorption coefficient for composites with different volume content of the metal fraction are shown in Fig. 6. Note that at the same frequencies, the absorption coefficient is greater for composites with a higher volume content of metal nanoparticles, regardless of their shape. Form of the curves $\eta(\hbar\omega)$ obeys the general laws described above.
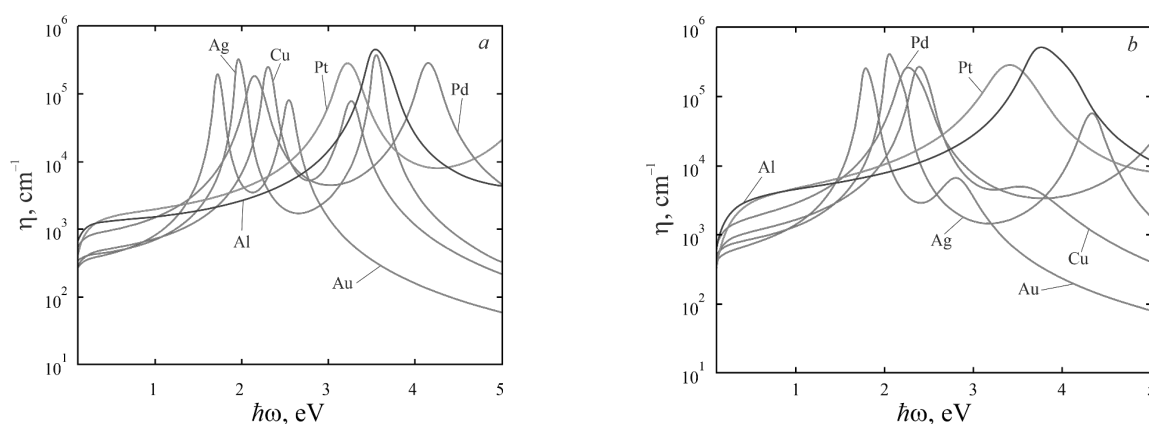

Fig. 4. Frequency dependences of the absorption coefficient of the composite with nanoparticles of various metals in Teflon: *a* – prolate spheroids ($a_t = 10$ nm, $b_l = 100$ nm); *b* – oblate spheroids ($a_t = 50$ nm, $b_l = 20$ nm)
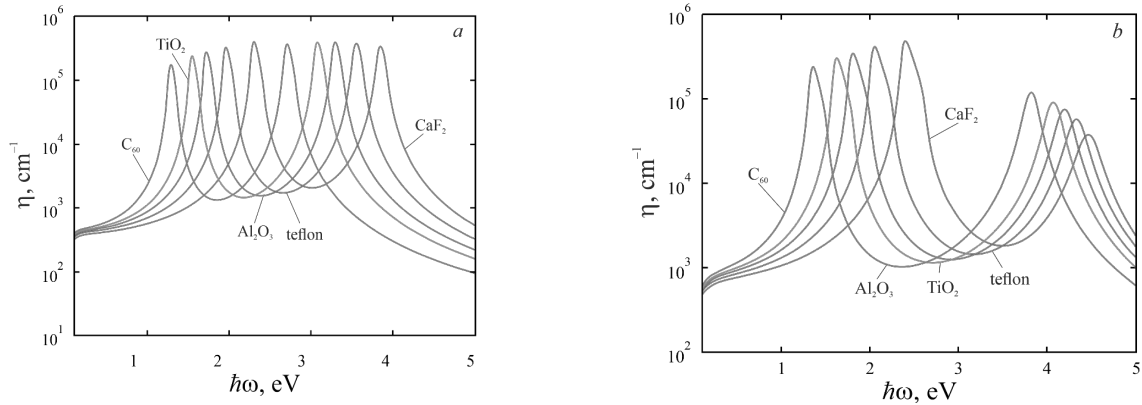
Fig. 5. Frequency dependences of the absorption coefficient of the composite with silver nanoparticles in different environments: a – prolate spheroids ($a_t = 10$ nm, $b_l = 100$ nm); b – oblate spheroids ($a_t = 50$ nm, $b_l = 20$ nm)
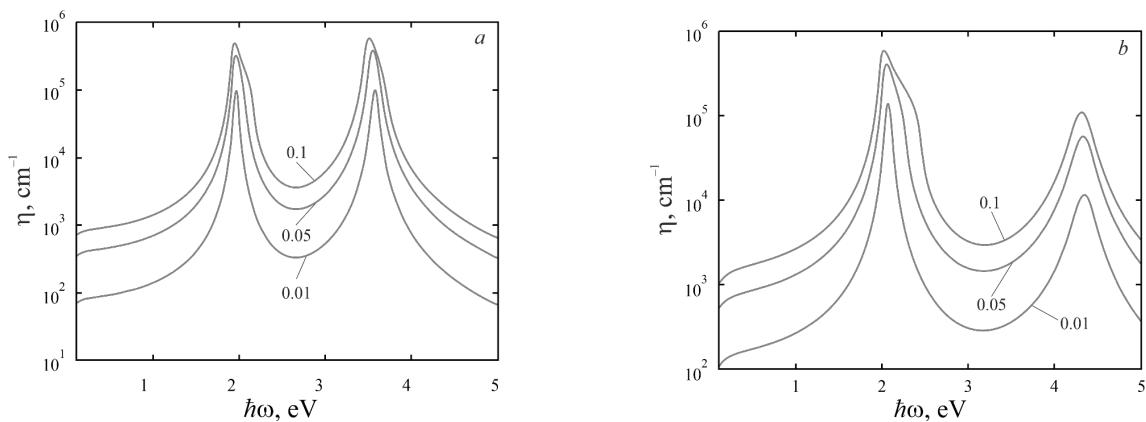

Fig. 6. Frequency dependences of the absorption coefficient of the composite with silver nanoparticles in Teflon at different values of volume content: a – prolate spheroids ($a_t = 10$ nm, $b_l = 100$ nm); b – oblate spheroids ($a_t = 50$ nm, $b_l = 20$ nm)

CONCLUSIONS

The relationship for the frequency dependences of the effective dielectric function and the absorption coefficient of the composite with metal nanosized particles-inclusions in the form of prolate and oblate spheroids was obtained.

It has been found that the distance between the maxima of the imaginary part of the effective dielectric function of the composite with inclusions of both shapes decreases as the shape of the particles approaches spherical, which is associated with the presence of two surface plasmon resonances in spheroidal particles and one in spherical particles. It can be assumed that the shape of the frequency dependence curves of the dielectric function is determined not by the length of the semi-axes separately, but by the eccentricity.

It is shown that the behavior of the maxima of the absorption coefficient upon a change in the form of inclusion particles is the same as the maxima of the effective dielectric function, and the maximum values of the absorption coefficient are larger in the case when the inclusions have the shape of an oblate spheroid.

It is proved that the change of the metal of inclusions and the matrix medium results in a shift of the maxima of the absorption coefficient, namely, a "blue" shift upon a decrease of dielectric permittivity and an increase in the frequency of volume plasmons.

It was demonstrated that the spectral position of the first maximum of the absorption coefficient of composites with inclusions of different metals, with different matrix media and volume content of inclusions does not depend on the type of spheroids, while the second maxima are shifted toward higher frequencies and smaller by two orders of magnitude in the case of flattened spheroidal nanoparticles.

Оптичне поглинання композитами з металевими нанорозмірними сфероїдальними частинками

Н.І. Павлище, А.В. Коротун, В.П. Курбацький

Національний університет «Запорізька політехніка»
вул. Жуковського, 64, Запоріжжя, 69063, Україна, andko@zp.edu.ua
Інститут металофізики ім. Г.В. Курдюмова Національної академії наук України
бульв. Академіка Вернадського, 36, Київ, 03142, Україна

У роботі розглядається задача про поглинання світла нанокомпозитом з хаотично орієнтованими металевими сфероїдальними частинками-включеннями за умови малого об'ємного вмісту таких включень. Отримано вирази для частотних залежностей ефективної діелектричної функції та коефіцієнта поглинання метал-діелектричного нанокомпозиту у рамках моделі ефективного середовища з урахуванням аксіальної симетрії сфероїдальних включень. Ефективну швидкість релаксації електронів введено з використанням кінетичного підходу. Числові розрахунки проведено для випадків, коли частинки-включення мають форму витягнутих і сплюснених наносфероїдів. Результати розрахунків свідчать про наявність двох максимумів коефіцієнта поглинання, які відповідають поздовжньому та поперечному поверхневому плазмонному резонансу. Проаналізовано зміну положення та величини максимумів частотних залежностей ефективної діелектричної функції та коефіцієнта поглинання при зміні розміру і форми сфероїдальних частинок-включень. Показано, що чим більшою є різниця довжин півосей сфероїдів, тим більшою є відстань між максимумами ефективної діелектричної функції і коефіцієнта поглинання, а форма кривих залежить від ексцентриситету сфероїдальних включень. Встановлено, що на положення максимумів суттєво впливає вибір матеріалу частинок включення та матричного середовища, тоді як на висоту максимумів значною мірою впливає форма наночастинок, а також їхній об'ємний вміст у композиційному середовищі. Доведено, що залежно від матеріалу наночастинок-включень, обидва максимуми коефіцієнта поглинання можуть знаходитися у видимій частині спектра (для включень Au) або в ультрафіолетовій (для включень Al). Можливо також, що один максимум лежить у видимій частині спектра, а інший – в ультрафіолетовій, що має місце для включень Pd, Pt, Cu, Ag.

Ключові слова: *нанокомпозит, витягнуті та сплюснені сфероїди, ефективна діелектрична функція, коефіцієнт поглинання, ефективна швидкість релаксації*

REFERENCES

1. Dmitruk N.L., Goncharenko A.V., Venger E.F. *Optics of small particles and composite media*. (Kyiv: Naukova Dumka, 2009).
2. Shang L., Bian T., Zhang B., Baihui Z., Zhang D., Wu L.-Z., Tung C.-H., Yin Y., Zhang T. Graphene-supported ultrafine metal nanoparticles encapsulated by mesoporous silica: robust catalysts for oxidation and reduction reactions. *Angew. Chem. Int. Ed.* 2014. **53**(1): 250.
3. *Nanocolloids: A Meeting Point for Scientists and Technologists*. Ed. by M. Sanchez-Dominguez and C. Rodriguez-Abreu (Elsevier, Amsterdam, 2016).
4. Levin V., Markov M., Mousatov A., Kazatchenko E., Pervago E. Effective electro-magnetic properties of microheterogeneous materials with surface phenomena. *Eur. Phys. J. B.* 2017. **90**(192): 1.
5. Mitra A., De G. *Glass Nanocomposites: Synthesis, Properties and Applications*. Chapter 6: Sol-gel synthesis of metal nanoparticle incorporated oxide films on glass. (Elsevier: William Andrew, 2016).
6. Xiang W., Gao H., Ma L., Ma X., Huang Y., Pei L., Liang X. Valence state control and thirdorder nonlinear optical properties of copper embedded in sodium borosilicate glass. *ACS Appl. Mater. Interfaces*. 2015. **7**(19): 10162.
7. Zhong J., Xiang W., Chen Z., Xie C., Luo L., Liang X. Microstructures and thirdorder optical nonlinearities of Cu_2In nanoparticles in glass matrix. *J. Alloys Compd.* 2013. **572**: 137.
8. Karmakar B. *Glass Nanocomposites: Synthesis, Properties and Applications.* Chapter 1: Fundamentals of glass and glass nanocomposites. (Elsevier: William Andrew, 2016).
9. Korgel B.A. Composite for smarter windows. *Nature*. 2013. **500**(7462): 278.

10. Llordés A., Garcia G., Gazquez J., Milliron D.J. Tunable near-infrared and visible-light transmittance in nanocrystal-in-glass composites. *Nature*. 2013. **500**(7462): 323.
11. Luan F., Gu B., Gomes A.S.L., Yong K.-T., Wen S., Prasad P.N. Lasing in nanocomposite random media. *Nano Today*. 2015. **10**(2): 168.
12. Kleemann W. Multiferroic and magnetoelectric nanocomposites for data processing. *J. Phys. D Appl. Phys*. 2017. **50**(22): 223001.
13. Barillaro G., Nannini A., Pieri F. APSFET: A new, porous silicon-based gas sensing device. *Sens. Actuators, B*. 2003. **93**(1–3): 263.
14. Dul S., Fambri L., Pegoretii A. *Structure and Properties of Additive Manufactured Polymer Components.* Development of new nanocomposites for 3D printing applications. (Elsevier: Woodhead Publishing, 2020).
15. Hauert R., Patscheider J. From alloying to nanocomposites-Improved performance of hard coatings. *Adv. Eng. Mater*. 2000. **2**(5): 247.
16. Shao H.-C., Zhang Y.-Y., Hussain S., Liu X.-C., Zhao L.-J., Zhang X.-Z., Liu G.-W., Qiao G.-J. Effects of Preform Structures on the Performance of Carbon and Carbon Composites. *Sci. Adv. Mater*. 2019. **11**(7): 945.
17. Kravets V.G., Kabashin A.V., Barnes W.L., Grigorenko A.N. Plasmonic Surface Lattice Resonances: A Review of Properties and Applications. *Chem. Rev*. 2018. **118**(12): 5912.
18. Lama P., Suslov A., Walser A.D., Dorsinville R. Plasmon assisted enhanced nonlinear refraction of monodispersed silver nanoparticles and their tunability. *Opt. Express*. 2014. **22**(11): 14014.
19. Golovan L.A., Timoshenko V.Y. Nonlinear-Optical Properties of Porous Silicon Nanostructures. *J. Nanoelectron. Optoelectron*. 2013. **8**(3): 223.
20. Rane A.V., Kanny K., Abitha V.K., Thomas S. *Synthesis of Inorganic Nanomaterials.* Chapter 5 - Methods for synthesis of nanoparticles and fabrication of nanocomposites. (Elsevier: Woodhead Publishing, 2018).
21. Hulkkonen H.H., Salminen T., Niemi T. Block Copolymer Patterning for Creating Porous Silicon Thin Films with Tunable Refractive Indices. *ACS Appl. Mater. Interfaces*. 2017. **9**(37): 31260.
22. Korotun A.V., Koval A.O., Reva V.I. Optical absorption of composite with bilayer nanoparticles. *J. Phys. Stud*. 2019. **23**(2): 2603.
23. Korotun A.V., Koval' A.A., Titov I.N. Optical Absorption of a Composite Based on Bilayer Metal–Dielectric Spherical Nanoparticles. *J. Appl. Spectrosc*. 2020. **87**(2): 240.
24. Grechko L.G., Motrych V.V., Ogenko V.M. Dielectric permeability of dispersed systems. *Surface*. 1993. **1**: 17. [in Ukrainian].
25. Landau L.D., Lifshitz E.M. *Course of Theoretical Physics*, V. 8: Electrodynamics of Continuous Media. (Pergamon, New York, 1984).
26. Korotun A.V., Pavlyshche N.I. Optical absorption of a composite with randomly distributed metallic inclusions of various shapes. *Funct. Mater*. 2022. **29**(4): 567.
27. Smirnova N.A., Maniuk M.S., Korotun A.V., Titov I.M. An optical absorption of the composite with the nanoparticles, which are covered with the surfactant layer. *Physics and Chemistry of Solid State*. 2023. **24**(1): 181.